

Evaluation of *in vitro* mutagenicity and genotoxicity of magnetite nanoparticles

Iman Omar Gomaa¹, Mahmoud Hashem Abdel Kader¹, Taher A. Salah Eldin², Ola Ahmed Heikal^{1,3,*}

¹ Faculty of Pharmacy and Biotechnology, German University in Cairo, Egypt;

² Nanotechnology Center, Regional Centre for Food and Feed, Agricultural Research Centre, Cairo, Egypt;

³ Narcotics, Ergogenics & Poisons Department, National Research Center, Giza, Egypt.

ABSTRACT: For successful application of nanomaterials in bioscience, it is essential to understand the biological fate and potential toxicity of nanoparticles. The aim of this study is to evaluate the genetic safety of magnetite nanoparticles (MNPs) (Fe_3O_4) in order to provide their diverse applications in life sciences, such as drug development, protein detection, and gene delivery. Concentrations of 10 ppm, 30 ppm, and 70 ppm (10-70 $\mu\text{g}/\text{mL}$) of the MNPs of 8.0 ± 2.0 nm were used. Characterization of MNPs was done with transmission electron microscopy (TEM), X-Ray Diffractometry (XRD) and a vibrating sample magnetometer (VSM). The MNPs mutagenic potential was evaluated using the Salmonella Ames test with Salmonella strains TA100, TA2638, TA102, and TA98 in the presence and the absence of metabolic activation with S9-liver extract. Genetic mutations at the chromosomal level and extent of DNA damage using the alkaline Comet assay were applied to peripheral blood lymphocytes and HEK-293 cell lines respectively. There were significant changes in the results of the Salmonella mutagenicity test at the 70 ppm concentration of MNPs which might reflect their mutagenic activity at higher concentrations. Cytogenetic evaluation revealed the absence of genetic mutations at the chromosomal level. The extent of DNA damage quantified by Comet assay and the mutagenicity study using Ames test were significantly correlated for the MNPs. Our results indicated that magnetite nanoparticles with the defined physicochemical properties caused apparent toxicity at higher concentrations of 30 ppm and 70 ppm without chromosomal abnormalities under the experimental conditions of this study.

Keywords: Magnetite nanoparticles, mutagenicity, genotoxicity, *in vitro* assays

*Address correspondence to:

Dr. Ola A. Heikal, Department of Pharmacology & Toxicology, Faculty of Pharmacy and Biotechnology, German University in Cairo, New Cairo City - Main Entrance Al Tagamoa Al Khames, Egypt.
E-mail: ola.heikal@guc.edu.eg

1. Introduction

Nanomaterial safety is becoming an increasingly debatable issue that has intensified over the past several years. The small size and particular shape, large surface area and surface activity, which make nanomaterials attractive in many applications, may contribute to their toxicological profile. Regarding their safety assessment nanomaterials cannot be treated in the same manner as chemical compounds. Therefore, the establishment of principles and test procedures to ensure the safe use of nanomaterials in the marketplace is urgently required. Magnetite nanoparticles (MNPs) are used with the intent to be utilized in bioscience for targeted delivery applications because they offer benefits such as separation and gathering of materials of interest in the presence of a magnetic force (*I*). Accordingly, for such a purpose, sufficient data regarding the toxicity and biological fate of the MNPs should be collected. In this study synthesized MNPs with an average size of 8.0 ± 2.0 nm were evaluated for their genotoxic effect to study their potential chronic toxicity, however the same particles were patented to be used as a single dose treatment for iron deficiency anemia and did not show any apparent toxicity on experimental animals during *in vivo* acute, sub-acute and chronic toxicity testing (2). Experience with non-nano substances taught us that mechanisms of genotoxic effects could be diverse. Application of standard genotoxic methods to nanomaterials and the interpretation of results are of highest consideration. Thus a practical approach is the use of a battery of standard genotoxicity testing methods covering wide ranges of mechanisms (3). In the presented work a comparative study for number of *in vitro* mutagenicity and genotoxicity investigations were performed including a bacterial reverse mutation test (Ames test), Single Cell Gel Electrophoresis assay (SCGE; comet assay), and standard karyotyping detection of chromosomal aberrations. Several studies on different types of synthesized MNPs have already proven their biocompatibility at the cellular level (4,5),

yet detection of gene mutation and DNA damage at the molecular level are still to be investigated.

Gentotoxicity studies on nanomaterials concluded that the particle size and charges, concentration, coating surfactant aggregation and surface properties of the nanoparticles, have profound influence on interpreting the genotoxicity testing. Small particle size (high surface area/mass) with high absorption capacity causes coating of the particles with proteins and nutrients from the culture media. This could obscure the essential nutrients for cell division in *in vitro* genotoxicity tests and influence cell proliferation leading to false positive results (6). In other cases, particles surface energy enhances catalytic activities leading to production of genotoxic reactive oxygen species. In the presented study, we tried to provide some characteristics of the chemical composition and physiochemical properties of the synthesized MNPs to draw a valid conclusion about their potential genetic side effects in comparison to other studies. Our aim is to help at improving our understanding of the underlying toxic mechanisms of MNPs. Such findings will have practical consequences in the risk assessment processes as well as the biomedical applications of these substances at the nanomaterials level.

2. Materials and Methods

2.1. Synthesis of biocompatible magnetite nanospheres

Magnetite nanospheres of 8.0 ± 2.0 nm were synthesized according to Jakubovic 1994 (7). In this work, water-soluble magnetite nanocrystals have been prepared *via* a co-precipitation reaction where 0.54 g of anhydrous ferric chloride (FeCl_3 , sigma-Aldrich, 99.99%) were dissolved in deionized water (Milli-Q Ultrapure Water System, Millipore) at room temperature. Zero point six gram sodium carbonate (Na_2CO_3 , BioXtra, $\geq 99.0\%$ Sigma-Aldrich) powder dissolved in deionized water is added to the FeCl_3 solution with continued stirring for 10 min, the solution turned viscous with a brown color. Directly 0.12 g ascorbic acid (99.0%, Sigma-Aldrich) as a reducing agent and a biocompatible capping material was added with vigorous stirring for 15 min, and the color of solution turned black. The solution was autoclaved at 120°C for 4 h then washed with deionized water three times to remove the excess of the non-reacted precursors. The synthesized magnetite nanoparticles (MNPs) were characterized by Transmission Electron Microscope (TEM, Tecnai G20, FEI), X-Ray Diffractometry (X'Pert Pro, PanAlytical) and a Vibrating Sample Magnetometer (VSM, Lakeshore 7400).

2.2. Toxicological evaluation of the synthesized MNPs in biological systems *in vitro*

Salmonella typhimurium TA100, TA2638, TA102, and

TA98 bacterial strains were purchased from Bonnie Kuenstler, Discovery Partners International Inc., San Diego, CA, USA and Trinova Biochem GmbH, Gießen, Germany. HEK-293 human embryonic kidney fibroblasts were obtained from the American Type Culture Collection (ATCC, CRL 1573). One million HEK-293 cells/mL were cultured in Eagle's MEM supplemented with 10% fetal bovine serum and L-glutamine (200mM). Cells were counted and treated with different concentrations of MNPs and the positive controls then incubated in the dark for either 1 h or 30 min at 37°C and 5% CO_2 .

In this work four different strains of the bacteria *S. typhimurium* were used. They differ in characteristic mutations in the *hisG* or *hisD* gene. Strains TA2638 and TA102 have a genotype mutation in *hisG428* while TA100 and TA 98 showed a mutation in *HisG46* and *His D3052* respectively. TA98 has a frame shift mutation, and all other strains show a base pair point mutation. Additionally, these strains have some other mutations that make them more susceptible to potential mutagens, using *S. typhimurium* mutants with a *rfa* – gene to increase the uptake of hydrophobic substances. The *uvrB* gene which is involved in DNA repair, guarantees the mutation would not be corrected by DNA repair machinery. Strains harbor the pKM101 plasmid that codes for ampicillin resistance to further improve the sensitivity of the assay.

Blood samples were collected in sterile heparinized vacutainer tubes and processed for Human Peripheral Lymphocytes (HPL) separation according to Singh *et al.*, (8). The lymphocyte layer seen as a buffy coat was aspirated and washed with PBS and then incubated overnight in RPMI growth medium containing 0.001% phytohemagglutinin. Equal numbers of cells were seeded in 24 well plates for testing each experimental condition. Cells were treated with different concentrations of MNPs and positive controls. Tested compounds were incubated with the cells in the dark for either 1 h or 30 min at 37°C and 5% CO_2 .

2.3. Ames mutagenicity test

The Salmonella mutagenicity assay was performed according to Maron *et al.*, 1983 (9), using *S. typhimurium* strains TA100, TA2638, TA102, and TA98. Benzo[a]pyrene; 0.1 mg/plate (Sigma-Aldrich) was used as a positive control for activity of cytochromes P450. Other positive controls were used including sodium azide, 1.5 $\mu\text{g}/\text{plate}$; 2-aminoanthracene (2-AA) 10.0 $\mu\text{g}/\text{plate}$ (Trinova Biochem, Germany), and cyclophosphamide, 0.2 mg/plate (Sigma-Aldrich). Positive controls were dissolved in deionized distilled water (DDW) or dimethylsulfoxide (DMSO). Bacterial cells were inoculated on NB-NaCl medium containing 75 $\mu\text{g}/\text{mL}$ ampicillin and 90 μM histidine

and cultured for 15 h at 37°C with continuous agitation at 150 rpm until the cell density became $1-2 \times 10^5$ /mL. Concentrations of 10 ppm, 30 ppm, and 70 ppm MNPs diluted in DDW were tested. DMSO was used as a reference negative control. All positive and negative controls as well as the MNPs concentrations were incubated at 37°C for 45 min with the bacterial cells in presence and absence of a 0.5 mL metabolic mixture containing subcellular fractions from male rat livers S9 liver extract (5% (v/v) in the metabolic mixture), (Sigma-Aldrich Chemie GmbH) using NADPH and G-6-P as cofactors (Sigma-Aldrich). The reaction mixture was then mixed with 2 mL top agar supplemented with 7 mM histidine (Sigma-Aldrich) and 5 mM biotin (Sigma-Aldrich) and then poured onto minimal glucose agar plates lacking histidine and allowed to harden. Agar plates containing treated bacterial strains were incubated at 37°C for 48 h, and the number of reverting colonies in the positive controls and the different dilutions of tested MNPs were counted and compared to those in the negative control.

2.4. *In vitro* comet assay in HEK-293 and HPL cells

Human embryonic kidney cells (HEK-293) and HPL cells from blood samples were used for the *in vitro* Comet assay investigation. A suspension of 10^6 cells prepared in 1 mL MEM fresh medium were incubated with the positive control compound (cyclophosphamide monohydrate) and the different dilutions of MNPs (10, 30, and 70 ppm MNPs diluted in DDW) at 37°C for 30 min and 1 h in the dark and in serum depleted medium in order to minimize DNA repair mechanisms. Cells incubated with PBS were used as a negative control. At the end of each incubation time, cells were washed twice with 1 mL PBS. Centrifugation was in the dark and cold at 1,400 rpm for 3 min. Viability of treated cells was determined using the trypan blue exclusion method and monitored at 75% with reference to the PBS treated cells in order to exclude cytotoxic effects in the interpretation of the assay results (10, 11). Treated cells were finally suspended in 200 μ L of 1.2% low melting point agarose (LMPA) at 37°C. Duplicate slides were prepared for each group of treated cells. One hundred μ L volumes of cell suspensions in LMPA were pipetted on each slide pre-coated with 0.6% normal melting point agarose (NMPA). Slides were covered with a suitable cover slip, and gels were allowed to solidify on an ice-cold surface for 15 min. Cells were incubated in the dark for 1 h at 4°C in lysis buffer (2 M NaCl, 100 mM EDTA, 10 mM Trizma base pH 10, freshly added 1% Triton X-100, and 10% DMSO). Slides were then washed three times with distilled water. Subsequently, the slides were incubated in an alkaline electrophoresis buffer (1 mM EDTA, 300 mM NaOH at pH 13) in an electrophoresis chamber (Thistle Scientific) for 30 min to allow the DNA to unwind and

then subjected to electrophoresis in the same buffer, for 30 min at 25 V and 300 mA. All electrophoresis steps were carried out in dark conditions followed by proper washing in neutralizing buffer (0.4 M Tris, pH 7.5) and finally staining with 0.001% 20 μ g/mL ethidium bromide solution diluted in water before being scored.

For scoring the comet results, duplicate slides were counted for each dose and positive control groups. A total number of 100 cells in each slide were examined using a fluorescent microscope (Carl Zeiss, Axiostar plus, 37081) connected to an image analysis system (CometImager, metasystems GmbH). Quantification of DNA damage was assessed as a percentage of damaged DNA migrating to the tail.

2.5. *In vitro* Karyotyping for HPL

Duplicate whole blood cultures from healthy female donors were set up using a 0.5 mL peripheral blood sample in RMPI medium supplemented with 20% FBS, containing (10 μ g/mL) phytohemagglutinin in order to stimulate mitotic division. Treatment with each MNP dilution took place for 3 h or 24 h before harvesting the metaphase chromosomes. The mitotic spindle fiber inhibitor colcemid (0.2 μ g/mL) was added 18 min prior to cell harvesting which was performed 72 h after culture initiation. Cells were incubated with 10 mL of hypotonic solution (0.56% KCl) followed by fixation in a solution of methanol: acetic acid (3:1, v/v). Replicate slides of metaphases were prepared from each culture representing different drugs or concentrations of MNPs. Slides were incubated overnight at 40°C in phosphate buffered saline (3.4 g/L K_2HPO_4 , PH 6.8) at 56°C for 10 min followed by Giemsa banding of Metaphase chromosomes for 10 min. One hundred metaphase cells from each treatment group were analyzed for chromosomal damage. All slides were coded and screened in random order.

Aberrations were identified according to Savage, 1976 (12) as chromosome and chromatid type damage. Displaced and un-displaced fragments separated by a non-staining region equal to or greater than the width of the chromatid were scored as deletions. Non-staining regions of less than the chromatid width were scored as gaps. Prior to mutational analysis and Karyotyping the mitotic index (MI) for each culture was estimated based upon 500 lymphocytes.

2.6. Statistical analysis

For each of the applied assays, data were expressed as mean \pm SE from three independent experiments using Graphpad Prism (San Diego, CA, USA). Data were subjected to statistical analysis by Tukey Multiple comparison ANOVA test with 95% confidence interval levels. Treatment groups were considered significantly different from the control group at a value of $p < 0.05$.

3. Results

3.1. Magnetite nanospheres characterization

In the current study, the co-precipitation method for preparation of magnetite nanocrystals was adapted to obtain uniform, a nearly spherical well-dispersed aqueous solution with perfect magnetite properties. Ascorbic acid was used to protect the trivalent ion from reduction giving better biocompatibility character in hydrated aqueous solution. The TEM images of the synthesized MNPs show an average size of 8.0 ± 2.0 nm with spherical shape (Figure 1). The formation of pure magnetite nanoparticles was confirmed by XRD analysis where only the magnetite phase pattern appeared with a cubic crystal structure (ICCD card: 04-0025683, High score plus) (Figure 2). Measurement of magnetic properties was done using

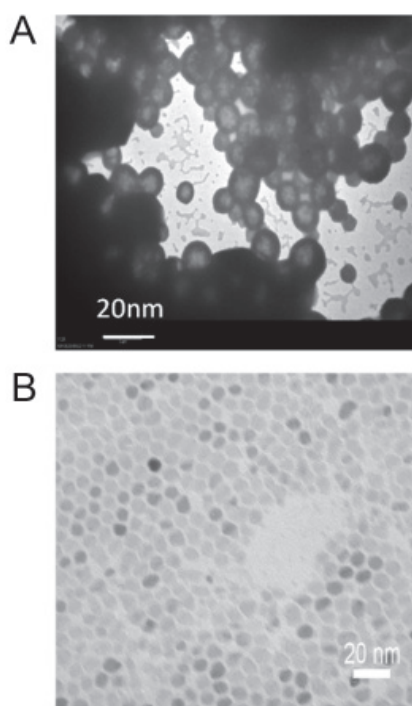


Figure 1. High power (A) and low power (B) TEM images of the MNPs capped with ascorbic acid showing that these particles have spherical shape with average size of 8.0 ± 2.0 .

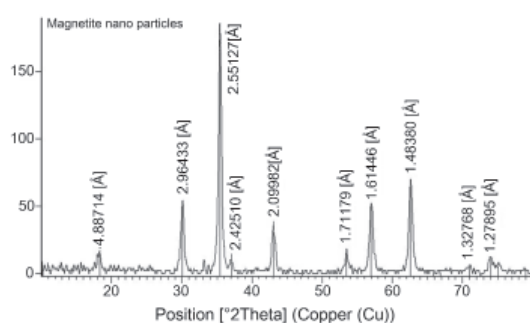


Figure 2. X-ray diffractometry (XRD) analysis of the magnetite phase pattern with cubic crystal structure.

VSM on an un-oriented, random assembly of particles at room temperature; a hysteresis loop was generated from which the intrinsic coercivity (H_c) remnant magnetization (M_r) and saturation magnetization (M_s) were calculated. The $M(H)$ curve or hysteresis loop for the magnetite sample measured under 15,000 Oe at room temperature is displayed in Figure 3. The saturation magnetization of the product is 5.2 emu/g and is much smaller than that (68.7 emu/g) of magnetite nanoparticles sized about 70 nm prepared through a hydrothermal method without any surfactant (13). In addition, the coercivity of synthesized magnetite approaches zero Oe indicating that the obtained magnetite nanoparticles are super paramagnetic.

3.2. MNPs mutagenic effect

The mutagenic effect of various MNP concentrations exerted on *Salmonella* strains with/without metabolic activation (S9 liver extract) were compared to negative control materials (water and DMSO) and positive control mutagenic agents benzo[a]pyrene, cyclophosphamide monohydrate, sodium azide, and 2AA. Results showed insignificant mutagenic activity ($p > 0.05$) for the MNPs at 10 ppm and 30 ppm concentration when incubated with all types of *Salmonella* strains in presence and absence of metabolic activation. On the other hand, 70 ppm of MNPs showed mutagenic activity only after metabolic activation, with TA100 ($p < 0.05$) compared to the negative control (Figure 4). Tested substances can reverse and correct *Salmonella* strains mutations to the wild type. It is known that TA100 and TA2638 strains may not detect certain oxidizing mutagens, cross-linking agents and hydrazines. Such substances may be detected by *S. typhimurium* TA102 which have an AT base pair at the primary reversion site.

3.3. MNPs DNA damage

The Comet assay was performed using the respective MNP concentrations after incubation with HEK 293 and

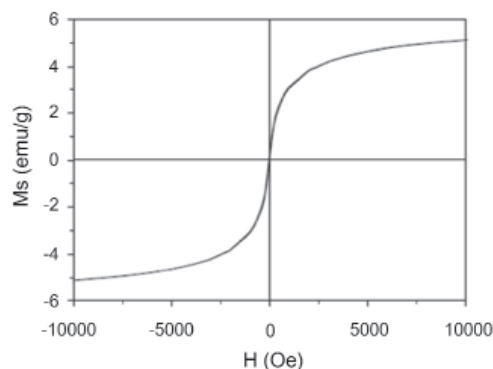


Figure 3. Hysteresis loop measurements of Fe_3O_4 nanoparticles capped with ascorbic acid proving its magnetic field properties.

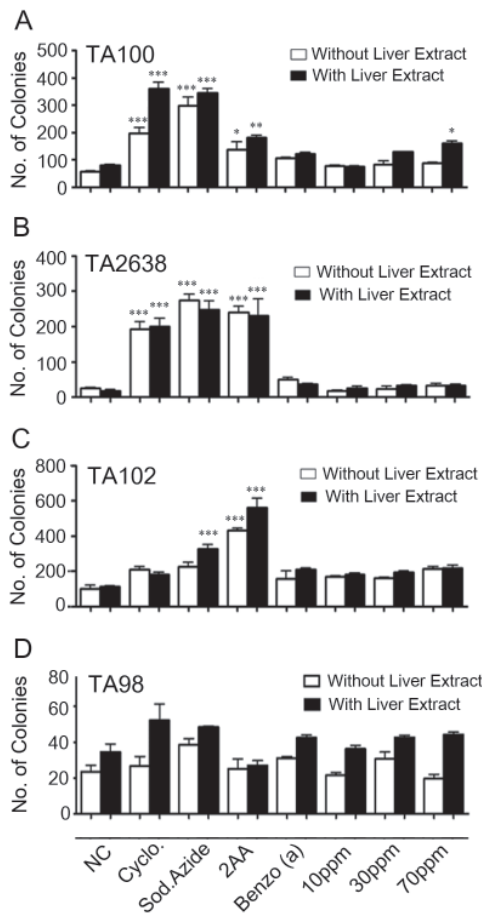


Figure 4. Mutagenic effect of MNPs in presence and absence of S9 liver extract. Results are reported as N° of revertant colonies with strains TA100 (A), TA2638(B), TA102 (C), and TA98 (D). Cyclophosphamide, sodium azide, 2-AA, and benzo (a) pyrene represent the positive controls. Results show the mean value + SE of three independent experiments. Significantly different from the control group at value of $p < 0.05$ (*), $p < 0.01$ (**), and $p < 0.001$ (***).

HPL cells for 30 min and 1h in comparison to a positive control; Cyclophosphamide monohydrate. The tail moment and % DNA damage data were expressed as mean \pm SE pooled from three independent experiments. No significant difference in tail moment measurements at MNP concentrations of 10 ppm and 30 ppm after 30 min were observed with HEK 293 cells nor HPL cells compared to the negative control ($p > 0.05$ vs. control), while a statistically significant increase in the tail moment was noticed at the maximum concentration of 70 ppm ($p < 0.01$). Exposure time up to 1 h showed a significant increase in the tail moment at 30 ppm and 70 ppm of MNPs with both types of cells (Figures 5A and 5B).

Genotoxicity level was measured as %DNA damage of HPL and HEK 293 cells after incubation with the three MNP concentrations. %DNA damage results showed an insignificant increase in genotoxicity at lower MNP concentrations (10 ppm and 30 ppm) at 30 min incubation. Significant genotoxicity was detected at all MNP concentrations after 1 h incubation with both types of cells (Figures 5C and 5D, Figure 6).

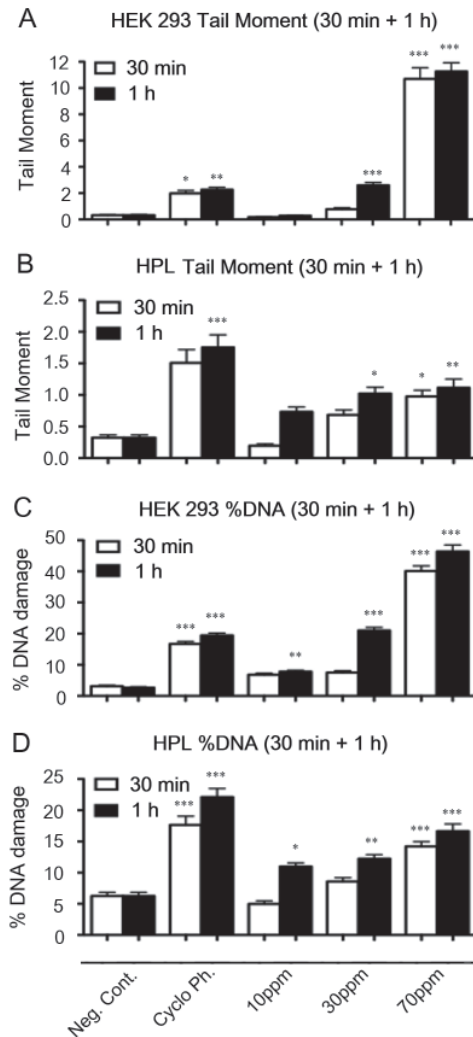


Figure 5. Genotoxic effect of MNPs after 30 and 60 min on HEK-293 cells (A, C) and HPL (B, D). Results are reported as tail moment and %DNA damage, respectively. Cyclophosphamide represents the positive control. Results show the mean value + SE of three independent experiments. Significantly different from the control group at value of $p < 0.05$ (*), $p < 0.01$ (**), and $p < 0.001$ (***).

3.4. Effect of MNPs on mitotic index and chromosomal structure

An *in vitro* cytogenetic test was carried out by treating human lymphocyte cultures with MNP concentrations using cyclophosphamide monohydrate as a positive control for both short term (3 h) and long term (24 h) incubation. Results at the short incubation time, revealed an absence of chromosome and chromatid types of mutation upon treating blood lymphocytes (HPL) with any of the MNP concentrations. Evaluation of the MNPs influence on the mitotic index proved that the mean percentages of mitotic indices after treatment with higher concentrations (30 ppm and 70 ppm) of MNPs for 3 h showed an insignificant decrease in mitotic index with the 30 ppm ($p > 0.05$) relative to a highly significant drop of metaphase count at 70 ppm ($p > 0.01$) in comparison to the control cells. However, at

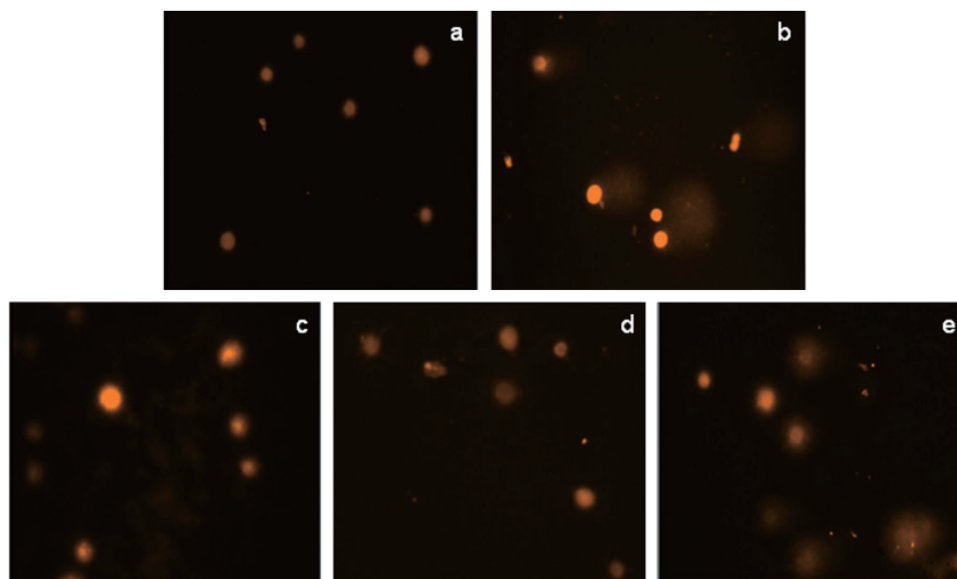


Figure 6. Comet images of HEK293 cells treated with PBS (a), cyclophosphamide (b), MNP concentrations of 10 ppm (c), 30 ppm (d), and 70 ppm (e).

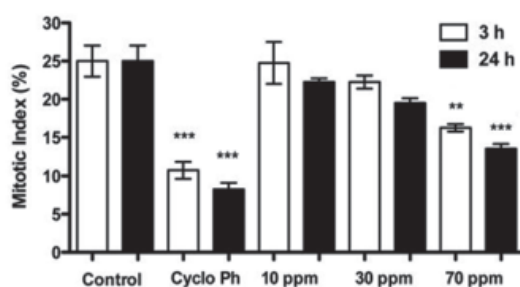


Figure 7. Mitotic index of human peripheral blood lymphocytes treated with different concentrations of MNPs at 3 h and 24 h. Results represented as % of the normal control. Cyclophosphamide represents the positive control. Results show the mean value + SE of three independent experiments. Significantly different from the control group at value of $p < 0.05$ (*), $p < 0.01$ (**), and $p < 0.001$ (***)

24 h results were significantly different for the 30 ppm ($p < 0.05$) and very highly significant in case of the 70 ppm ($p < 0.001$) compared to the non-treated control cells (Figure 7). Treatment of blood lymphocytes with (100 $\mu\text{g}/\text{mL}$) of cyclophosphamide for 3 h resulted in structural chromosomal aberrations in the form of breaks and gaps of both the chromatid and chromosome types with reference to the non-treated cells (Figure 8). However, extending the MNP incubation period to 24 h showed hypoploidy for several chromosome numbers in all examined metaphases. Accordingly, results of the mitotic index reflected severe suppression upon treatment with the MNPs both at 3 h and 24 h incubation times as indicated by extremely a significant decrease in mitotic indices in comparison to the untreated cells ($p < 0.001$) at both incubation periods.

4. Discussion

The present findings proved that MNPs had

concentration dependent and a reproducible pattern suggesting a mutagenic effect of synthesized MNPs with the *S. typhimurium* strains used under the present experimental conditions. Results obtained with the Ames test and Comet assay recorded high consistency. The intensity of DNA strand breaks measured as tail moment and/or %DNA damage were well correlated and were greater at 1 h incubation than at 30 min incubation. Maximum DNA migration was observed at 70 ppm MNP concentration after 1 h incubation. Detection of DNA migration after 1 h supports reported publications on the optimal detection time in Comet assay being less than 3 h for DNA damage observation. Otherwise, false negative results could be obtained as a result of DNA repair initiation (14). In comparison to our study, Sun *et al.* reported the effect of magnetite Fe_3O_4 particles with a size range (8-20 nm) using a 10-fold increase in concentration (0.1-4.6 mg/mL) as compared to ours (5). The Sun *et al.*, study on 3T3 monkey cells indicated the absence of a cytotoxic effect but didn't confirm the lack of a genotoxic effect. Our results also showed no cytotoxic effect with high cell viability (more than 75%) at lower MNP concentrations but evidenced a genotoxic effect. Thus it could be concluded that the MNP concentrations used, although not cytotoxic were significantly genotoxic especially at 70 ppm concentration. Comparison of our results to those of Sun *et al.* is difficult due to dissimilarity in the nanoparticles surface charge and composition characterization that could lead to different biological responses; however both cytotoxicity and genotoxicity should be conducted to confirm nanoparticle biocompatibility.

Results of the standard karyotyping revealed suppression of the mitotic index after incubation with the higher MNP concentrations (30 and 70 ppm).

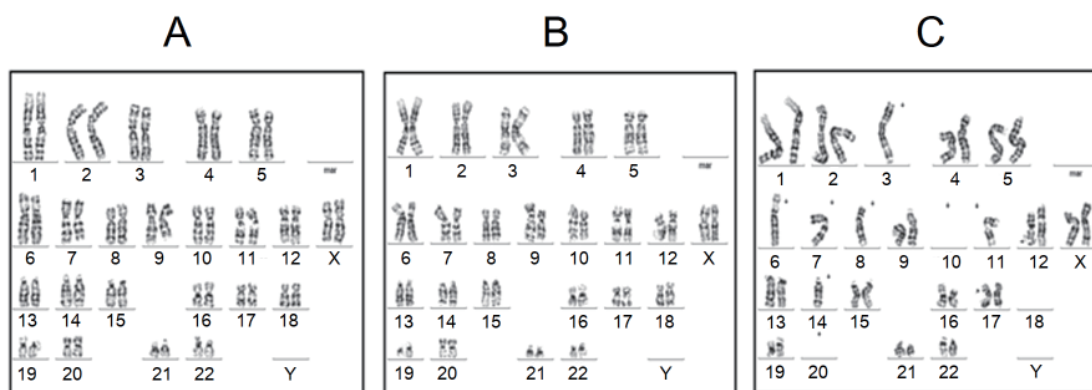


Figure 8. G-banded human Karyotypes of normal control cells (A), MNP treated cells (B), and cyclophosphamide (C), showing chromosomal breaks and fragments.

These concentrations of MNP induce mitotic cell arrest followed by cell death. This could be explained on the basis of extension in interphase due to inhibition of DNA synthesis and an increase in G1 phase duration (15). On the other hand, it might also be traced back to inhibition of some metabolic events necessary for the normal sequence of mitosis (16), or inhibition of protein synthesis (17).

In the present study, in spite of the fact that MNPs showed neither chromatid nor chromosome types of mutations, they could still be considered as clastogenic agents. In support of this, data obtained from the Comet assay as well as Ames test revealed that higher concentrations of MNPs exhibited significant genotoxic and mutagenic effects as compared to non-treated cells. Discrepancies in the results of the assays used might rely in one part on the test sensitivity as certain types of mutations such as sister chromatid exchange cannot be detected except with the application of more sensitive molecular techniques such as multiplex fluorescent in situ hybridization (mFISH) (18) which we intend to undertake in future studies.

For most nanoparticles it is unknown whether they directly interact with DNA as association of gold nanoparticles with the major groove of DNA (19) or indirectly through an inflammation mediated oxidative stress effect. Recognition of the oxidative DNA strand break in terms of FPG (formamidopyrimidine glycosylate) sensitive sites which cleaves DNA sites at the oxidized 8-oxoguanine purines has been reported in bronchoalveolar lavage cells from rats instilled with TiO₂ (20). In another study, iron nanoparticles were reported to be redox reactive with a pro-inflammation and pro-oxidative effect on various cell models (21,22). Since the mechanism underlying the interaction of DNA with iron nanoparticles has not been investigated yet, their elucidation can be demanding. Future studies on the exact interaction mechanism of iron nanoparticles with DNA are under investigation in our laboratories.

In conclusion, this work highlights that *in vitro* cytotoxicity testing of nanomaterials does not imply safety and biocompatibility as has been reported in

previous studies. We rather suggest an urgent demand for applying a battery of genotoxicity testing to assess the genotoxic hazard of nanoparticles. Information on the full characterization of the chemical composition and physiochemical properties of MNPs is important to elucidate the uptake potential in individual cell lines and how the particles will interact electrostatically with DNA and proteins in biological fluids to elucidate the underlying mechanism. Recognition of the genotoxic mechanism will improve the possibility of optimal choice of applied genotoxicity tests.

Future recommendations are directed towards investigation of the mutagenicity and genotoxicity of MNPs in *in vivo* model systems. This is due to the general belief that the positive results at the *in vitro* level are too extreme to be taken as an indication in terms of human exposure. The reason for that is pharmacokinetics, metabolism, tissue and species specificity may all play an important role in the *in vivo* genotoxicity and clastogenicity assays of different shapes, sizes, and chemical compositions of nanomaterials (23).

References

1. Hongwei G, Pak LH, Kenneth WT, Ling W, Bing X. Using biofunctional magnetic nanoparticles to capture vancomycin-resistant enterococci and other gram-positive bacteria at ultralow concentration. *J Am Chem Soc.* 2003; 125:15702-15703.
2. Salah TA, Baker MM, Kamel HM, Abdel Kader MH. Magnetite nanoparticles as a single dose treatment for iron deficiency anemia. 2010; PCT, WO 2010/034319 A1.
3. Landsiedel R, Kapp MD, Schulz M, Wiench K, Oesch F. Genotoxicity investigation on nanomaterials: Methods, preparations and characterization of test material, potential artifacts and limitations-Many questions, some answers. *Mutat Res.* 2009; 681:241-258.
4. Schwertmann U, Cornell RM. Iron oxides in the laboratory: Preparation and characterization, General preparative Techniques (Chapter 2). Weinheim; Chichester: Wiley-VCH, 2000; pp. 19-25.
5. Sun J, Zhou S, Hou P, Yang Y, Weng J, Li X, Li M. Synthesis and characterization of biocompatible Fe₃O₄

- nanoparticles. *J Biomed Mater Res A*. 2007; 80:333-341.
6. Guo L, Von Dem Bussche A, Buechner M, Yan A, Kane AB, Hurt RH. Adsorption of essential micronutrients by carbon nanotubes and implications for nano-toxicity testing. *Small*. 2008; 4:721-727.
 7. Xuan S, Hao L, Jiang W, Gong X, Hu Y, Chen Z. Preparation of water-soluble magnetite nanocrystals through hydrothermal approach. *J Magn Magn Mater*. 2007; 308:210-213.
 8. Singh NP, McCoy MT, Tice RR, Schneider EL. A simple technique for quantitation of low levels of DNA damage in individual cells. *Exp Cell Res*. 1988; 175:184-191.
 9. Maron DM, Ames BN. Revised method for the *Salmonella* mutagenicity assay. *Mutat Res*. 1983; 113:173-215.
 10. Anderson D, Plewa MJ. The international Comet assay workshop. *Mutagenesis*. 1998; 13:67-73.
 11. Henderson L, Wolfreys A, Fedyk J, Bourner C, Wndebank S. The ability of the comet assay to discriminate between genotoxins and cytotoxins. *Mutagenesis*. 1998; 13:89-94.
 12. Savage JRK. Annotation: Classification and relationships of induced chromosomal structural changes. *J Med Genet*. 1976; 13:103-122.
 13. Wang J, Chen Q, Zeng C, Hou B. Magnetic-field-induced growth of single crystalline Fe₃O₄ nanowires. *Adv Mater*. 2004; 16:137-140.
 14. Giannotti E, Vandin L, Repeto P, Comelli R. A comparison of the *in vitro* Comet with the *in vitro* chromosome aberration assay using whole human blood or Chinese hamster lung cells: Validation study using range of novel pharmaceuticals. *Mutagenesis*. 2002; 17:163-170.
 15. O'Connor PM, Ferris DK, Pagano M, Draetta G, Pines J, Hunter T, Longo DL, Kohn KW. G2 delay induced by nitrogen mustard in human cells affects cyclin A/cdk2 and cyclin B1/cdc2-kinase complexes differently. *J Biol Chem*. 1993; 268:8298-8303.
 16. Kamada NM, Shakurai M, Miyamoto K, Sanada I, Sadamori N, Fukuhara S, Sabe S. Chromosome abnormalities in adult T-cell Leukemia/lymphoma: A karyotype review committee report. *Cancer Res*. 1992; 52:1481-1493.
 17. Kane RS, Stroock AD. Nanobiotechnology: Protein nonmaterial interaction. *Biotechnol progr*. 2007; 23:316-319.
 18. Martín M, Terradas M, Iliakis G, Tusell L, Genescà A. Breaks invisible to the DNA damage response machinery accumulate in ATM-deficient cells. *Genes Chromosomes Cancer*. 2009; 48:745-759.
 19. Pan Y, Neuss S, Leifert A, Fischer M, Wen F, Simon U, Schmid G, Brandau W, Jahnen-Dechent W. Size dependent cytotoxicity of gold nanoparticles. *Small*. 2007; 3:1941-1949.
 20. Rehn B, Seiler S, Rehn S, Bruch J, Maierd M. Investigations on the inflammatory and genotoxic lung effect of two types of titanium dioxide: Untreated and surface treated. *Toxicol Appl Pharmacol*. 2003; 189:84-95.
 21. Stroh A, Zimmer C, Gutzeit C, Jakstadt M, Marschinke F, Jung T, Pilgrim H, Grune T. Iron oxide particles for molecular magnetic resonance imaging cause transient oxidative stress in rat macrophages. *Free Radic Biol Med*. 2004; 36:976-984.
 22. Edmond K, Baarine M, Pelloux S, Marc Riedinger J, Froulin F, Tourneur Y, Lizard G. Iron nanoparticles increase 7-ketocholesterol-induced cell death, inflammation, and oxidation on murine cardiac HL1-NB cells. *Int J Nanomedicine*. 2010; 5:185-195.
 23. Giri AK, Banerjee S. Genetic toxicology of four commonly used benzodiazepines: A review. *Mutat Res*. 1996; 340:93-108.
- (Received March 18, 2013; Revised May 22, 2013; Accepted May 30, 2013)